Original Article

Optimizing prostate biopsy decision-making for patients with Prostate Imaging-Reporting and Data System (PI-RADS) ≥3 lesions: novel magnetic resonance imaging (MRI)-based nomograms

Yanling Chen[1#], Jinhua Lin[2#], Wenxin Cao[1#], Tiebao Meng[3], Jian Ling[4], Zhihua Wen[1], Lingmin Kong[1], Long Qian[5], Yan Guo[1], Weijing Zhang[3], Huanjun Wang[1]

[1]Department of Radiology, The First Affiliated Hospital, Sun Yat-Sen University, Guangzhou, China; [2]Department of Medical Ultrasound, Division of Interventional Ultrasound, The First Affiliated Hospital, Sun Yat-sen University, Guangzhou, China; [3]Department of Radiology, Sun Yat-sen University Cancer Center, Guangzhou, China; [4]Department of Radiology, The Eastern Hospital of The First Affiliated Hospital, Sun Yat-Sen University, Guangzhou, China; [5]Department of Biomedical Engineering, College of Engineering, Peking University, Beijing, China

Contributions: (I) Conception and design: Y Chen, H Wang, W Zhang, Y Guo; (II) Administrative support: H Wang, W Zhang, Y Guo; (III) Provision of study materials or patients: J Lin, J Ling; (IV) Collection and assembly of data: W Cao, Z Wen, T Meng; (V) Data analysis and interpretation: Y Chen, L Qian; (VI) Manuscript writing: All authors; (VII) Final approval of manuscript: All authors.

[#]These authors contributed equally to this work as co-first authors.

Correspondence to: Huanjun Wang, MD. Department of Radiology, The First Affiliated Hospital, Sun Yat-Sen University, No. 58 Zhongshan Road 2, Guangzhou 510080, China. Email: wanghj45@mail.sysu.edu.cn; Weijing Zhang, MD. Department of Radiology, Sun Yat-sen University Cancer Center, No. 651 Dongfeng East Road, Guangzhou 510060, China. Email: zhangwj@sysucc.org.cn; Yan Guo, MD. Department of Radiology, The First Affiliated Hospital, Sun Yat-Sen University, No. 58 Zhongshan Road 2, Guangzhou 510080, China. Email: gyan@mail.sysu.edu.cn.

Background: Current protocols endorse biopsies for men with Prostate Imaging-Reporting and Data System (PI-RADS v2.1) scores ≥3. However, the subjective nature of PI-RADS can lead to increased false positives and unnecessary biopsies. Synthetic magnetic resonance imaging (MRI), which quantifies multiple relaxation parameters, and apparent diffusion coefficient (ADC), which is the most commonly used quantitative metric, have not yet been combined with a predictive tool. This study aimed to develop and validate novel nomograms using multiparametric MRI, including synthetic MRI, to forecast the risk of prostate cancer (PCa) and clinically significant prostate cancer (csPCa), and to assess the potential of these nomograms to reduce unnecessary biopsies in PI-RADS ≥3 cases.

Methods: Between August 2020 and August 2022, 323 patients suspected of PCa were enrolled from two centers (cohort 1: 243; cohort 2: 80). All participants underwent multiparametric MRI, including synthetic MRI, before targeted biopsy. Univariable and multivariable logistic regression identified risk factors for PCa and csPCa. Internal validation was conducted using bootstrap resampling, and nomogram performance was evaluated through receiver operating characteristic (ROC) curve analysis, calibration plots, and decision curve analysis (DCA). External validation was performed with cohort 2 data. The impact of the nomograms on biopsy decisions was measured by the avoidance rate and the risk of missed diagnoses.

Results: The predictive nomogram for PCa incorporated four risk factors: age, quantitative transverse relaxation time (T2 value) from synthetic MRI, ADC value, and PI-RADS score. The csPCa nomogram included age, ADC value, and PI-RADS score. The nomograms showed high diagnostic accuracy with the area under the curves (AUCs) of 0.916 [95% confidence interval (CI): 0.901–0.974] and 0.947 (95% CI: 0.900–0.994) for PCa prediction in training and external datasets, and 0.884 (95% CI: 0.840–0.928) and 0.935 (95% CI: 0.871–0.998) for csPCa. Calibration curves confirmed the accuracy of predictions. DCA indicated

that the nomograms possessed significant net benefit. For PCa detection, biopsy strategy combining our nomogram reduced biopsy procedures by 20.2% and 13.8% in the training and external cohorts, respectively, with a PCa miss rate of 4.5% for both cohorts. The csPCa-targeted biopsy strategy also provided clinical benefits, with biopsy avoidance rates of 20.2% and 10.0%, and csPCa miss rates of 4.8% and 1.7% for PI-RADS ≥3 patients in the two cohorts.

Conclusions: The nomograms integrating multiparametric MRI and synthetic MRI are highly effective in predicting PCa and csPCa, concurrently, reducing unnecessary biopsies for patients with PI-RADS ≥3 lesion.

Keywords: Multiparametric magnetic resonance imaging (multiparametric MRI); synthetic resonance imaging (synthetic MRI); prostate cancer (PCa); nomogram; prostate biopsy

Submitted May 29, 2024. Accepted for publication Aug 29, 2024. Published online Oct 11, 2024.
doi: 10.21037/qims-24-1072
View this article at: https://dx.doi.org/10.21037/qims-24-1072

Introduction

Globally, prostate cancer (PCa) becomes the second leading cause of death among men (1). With the widespread use of prostate specific antigen (PSA) screening, PCa is being detected at an earlier and more localized stage (2). However, it has also led to lots of unnecessary prostate biopsies and the unwanted post-biopsy complications due to the the low specificity of PSA (3). Multiparametric magnetic resonance imaging (MRI) has become an essential component of the diagnostic pathway for PCa. The clinical application of multiparametric MRI has improved the diagnosis of PCa and clinically significant prostate cancer (csPCa) (4). The Prostate Imaging Reporting and Data System (PI-RADS) was developed to standardize the acquisition and interpretation of multiparametric MRI images (5). Current guidelines recommend biopsies for men with a moderate (PI-RADS 3) to high likelihood (PI-RADS 4/5) of developing PCa (6-8) so as to curb the excessive biopsies. However, the clinical implementation of this strategy is hindered by moderate interreader and intercenter reproducibility, which can result in increased false-positive rates and unnecessary prostate biopsy (9-11). The integration of additional laboratory indices, clinical factors, or quantitative multiparametric MRI metrics may help address these limitations and identify patients who can safely avoid biopsies.

Synthetic MRI is an emerging technique that synthesizes magnetic resonance images at arbitrary contrast after the actual MRI scan, which can provide absolute quantification of longitudinal relaxation time (T1), transverse relaxation time (T2), and proton density (PD) maps simultaneously in a single scan within a short examination time. These quantitative values represent the intrinsic magnetic properties of the tissue and are independent of the MRI scanner or scanning parameters at a given field strength (12). This technique has shown excellent correlation with conventional mapping technique with no inferiority of image quality compared with that of conventional contrast-weighted images (12). Previous studies have demonstrated the feasibility of synthetic MRI in the diagnosis of breast cancer (13,14), bladder cancer (15) and some neurological diseases (16,17). In the field of PCa research, the diagnostic value of synthetic MRI has been affirmed for the evaluation of tumor activity in primary PCa as well as bone metastases of PCa. Both T1 and T2 values are the useful parameters in differentiating PCa from other benign lesions that can be easily confused with PCa in clinical practice (12). Additionally, the apparent diffusion coefficient (ADC) that derived from diffusion weighted imaging (DWI), is a common quantitative metric that has shown substantial ability in the detection of PCa.

Nomograms offer a unique capability of converting complex regression equations into visual graphs. Nomograms are known for their intuitive and user-friendly nature, making it increasingly popular and applicable in medical research and clinical practice (18). This study was conducted with the aim of developing and externally validating nomograms that integrate synthetic MRI and ADC metrics, thereby enhancing the identification of PCa and csPCa in men with PI-RADS ≥3 lesions. Furthermore, biopsy avoidance strategies based on the nomogram were proposed, and their efficacy in reducing unnecessary biopsies was evaluated. We present this article in accordance with the TRIPOD reporting

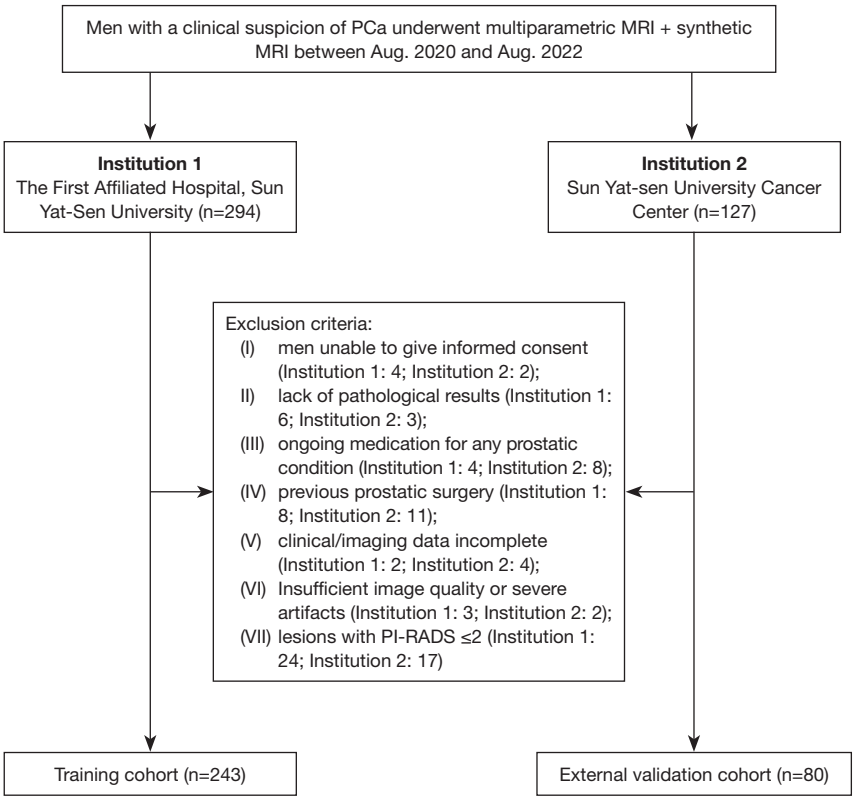

Figure 1 Flow chart of patient selection. PCa, prostate cancer; MRI, magnetic resonance imaging; PI-RADS, Prostate Imaging Reporting and Data System.

checklist (available at https://qims.amegroups.com/article/view/10.21037/qims-24-1072/rc).

Methods

Study populations

From August 2020 to August 2022, men suspected of PCa (elevated PSA level, suspicious digital rectal examination findings, or suspicious lesions on ultrasound examination) from two medical centres (Institution 1: The First Affiliated Hospital of Sun Yat-Sen University; Institution 2: Sun Yat-sen University Cancer Center) were referred for further evaluation. Patients who underwent prostate multiparametric MRI and synthetic MRI before prostate biopsy or radical prostatectomy without a prior diagnosis of PCa were included. The exclusion criteria were as follows: (I) lack of pathological results; (II) ongoing or previous medication for any PCa; (III) unavailable or incomplete clinical/imaging data; (IV) insufficient image quality with severe artefacts; and (V) lesions with PI-RADS ≤2. A flowchart of patient selection is detailed in *Figure 1*. The retrospective study was mainly designed and developed in The First Affiliated Hospital of Sun Yat-Sen University and ethical approval was obtained from the Ethics Committee of The First Affiliated Hospital of Sun Yat-Sen University (2023; approval No. 094). Both participating medical centres were informed and agreed with the study. Study participants provided written informed consent. The study was conducted in accordance with the Declaration of Helsinki (as revised in 2013).

Imaging acquisition

All MRI examinations were performed using a 3.0 T MRI scanner (Signa Pioneer, GE, IL, USA) equipped with a 32-channel coil. The conventional multiparametric MRI protocols included the following sequence: (I) axial T1-weighted imaging (T1WI); (II) axial, coronal, sagittal T2-weighted imaging (T2WI); and (III) axial DWI images (b values of 50, 1,000 and 1,500 s/mm^2). ADC maps

were automatically generated from the DWI images (b values of 50 and 1,000 sec/mm^2) on the scanner console. (IV) Dynamic contrast-enhanced imaging. Synthetic MRI was performed using a multidynamic multiecho (MDME) sequence. The quantitative parametric maps (T1, T2, and PD maps) were generated using vendor-provided offline postprocessing software (SyMRI7.2; Synthetic MR, Linköping, Sweden). The scanners and scan parameters remained consistent in the two centres. Detailed information about the aforementioned imaging sequences is presented in Table S1.

Image analysis

For all patients, prior to targeted biopsies, two experienced radiologists (Y.G. and J.L. with 30 and 15 years of experience in prostate MRI, respectively) independently interpreted the multiparametric MRI findings according to the PI-RADS guidelines (version 2.1), and a PI-RADS score was assigned to the cancer-suspicious lesion. Discrepancies between readings were solved through consensus.

For synthetic MRI, the volume of interest (VOI) of the whole tumour was manually delineated independently by two radiologists (Y.C. and W.C. with 4 years and 2 years of experience in prostate imaging, respectively) who were blinded to the clinical information and pathological results on the synthetic T2WI. The delineation was then replicated at the corresponding locations on the T1 and PD maps. For the ADC value, a free-hand VOI was drawn on the ADC map along the border of the whole tumour. Susceptibility artefacts, areas of haemorrhage and adjacent nonneoplastic structures were avoided. The average T1, T2, PD, and ADC values were automatically calculated in the VOI for each participant. The average values of the two radiologists were used for analysis. All radiologists were blinded to the pathological result but not the lesion location on MRI images. VOI drawing was conducted using ITK-SNAP software (version 2.2.0; www.itksnap.org).

Histopathologic analysis and correlation with MRI

For patients who underwent radical prostatectomy, postoperative pathological results were considered to be the reference standard; otherwise, the results of prostate biopsy were adopted. The biopsy procedure was performed at each centre by experienced urologists with at least five years of prostate biopsy experience (>300 cases of prostate biopsy each). All patients underwent transperineal or transrectal ultrasound-guided cognitive target biopsies. At least 2 target cores were obtained in the suspicious areas. Then, all specimens were reviewed at the two medical centres, according to the International Society of Urological Pathology (ISUP) grading standards, by seasoned uropathologists who were blinded to the clinical information and imaging results of the patients. The pathological type of lesion was recorded as cancer, prostatitis, benign prostatic hyperplasia (BPH), or benign prostate tissue. For PCa, the highest ISUP grade group for each lesion was also documented. PCa referred to lesion with ISUP grade group ≥1, and csPCa was defined as ISUP grade group ≥2 (19).

The index lesion was defined as the lesion with the highest PI-RADS score. If more than one lesion had the same PI-RADS score, then the largest lesion was selected. To realize the radiologic-pathologic matching of lesions, for patients who underwent prostate biopsy, the final histopathologic diagnosis was determined by correlating the lesion location on MRI images with the location descriptions on the cognitively targeted core pathology reports. For patients who underwent radical prostatectomy, pathological confirmation was determined by mapping lesion annotations from histopathologic slices onto the prostate MRI scans.

Statistical analysis

The Kolmogorov-Smirnov or Shapiro-Wilk test and Levene's test were performed to evaluate the normality and homoscedasticity of continuous data, respectively. Continuous data were expressed as the mean ± standard deviation or median (first quartile, third quartile) and were compared with Student's *t*-test or the Mann-Whitney U test depending on the distribution and homoscedasticity of the data. Categorical variables were described as numbers (rates), and the Chi-squared test was used for comparisons between different groups. The enrolled patients from The First Affiliated Hospital of Sun Yat-Sen University were assigned to training cohort and patients from Sun Yat-sen University Cancer Center were allocated to the external validation dataset. A boot strapping method with 1,000 replications was used for internal validation. Univariate and multivariate logistic regression were conducted based on data from the training cohort to identify independent risk factors for PCa and csPCa, which were then incorporated into the final nomograms. Performance evaluation for the nomogram included discrimination, calibration, and

clinical utility in all three cohorts. Discriminatory ability was measured with receiver operating characteristic (ROC) curve analysis and the generating area under the curve (AUC). Model calibration was visually assessed by using calibration curves and quantitatively evaluated by the Hosmer-Lemeshow test, with a P value greater than 0.05 considered satisfactory. Clinical utility was assessed via decision curve analysis (DCA).

Based on the ROC curve of the developed nomograms, a cut-off value with a positive likelihood ratio (LR+) ≥10 and specificity ≥95% was designated as the boundary value of the high-risk threshold, and a cut-off value with a negative likelihood ratio (LR–) ≤0.1 and sensitivity ≥95% was defined as the low-risk threshold. The above criteria were then applied to the novel biopsy strategies, then the biopsy avoidance rate, PCa missed rate as well as csPCa missed rate were calculated to assess their potential impact on biopsy decisions. The unnecessary biopsy avoidance rate in men with PI-RADS category 3 lesions was also calculated.

Interrater variability of T1, T2, PD, and ADC value measurement were assessed using the intraclass correlation coefficient (ICC), which was classified as excellent (≥0.80), good (0.60–0.79), fair (0.40–0.59), and poor (<0.40). Statistical analyses were conducted using statistical software, including SPSS (v.26.0, IBM), MedCalc (v.12.7; www.medcalc.org), and R (v.4.1.1. http://www.r-project.org/). A two-sided P<0.05 was considered statistically significant.

Results

Patient characteristics

A total of 243 patients from The First Affiliated Hospital of Sun Yat-Sen University and 80 patients from Sun Yat-sen University Cancer Center were included. Among these men, 184 underwent biopsy, and 139 underwent radical prostatectomy. The prevalence of PCa and csPCa was 73.3% (178 out of 243 patients) and 68.3% (166 out of 243 patients) in the training cohort and 82.5% (66 out of 80 patients) and 73.8% (59 out of 80 patients) in the external validation cohort, respectively. All patient data, including demographic, clinical and imaging features, from the two institutions are presented in *Table 1*.

Interreader reliability

The interreader reliabilities were good-to-excellent for T1, T2, PD and ADC in the two cohorts. The ICCs for the aforementioned parameters are summarized in Table S2.

Nomogram establishment

In the training cohort, older age, higher total prostate-specific antigen (tPSA) and higher free prostate-specific antigen (fPSA) were observed in patients with PCa or csPCa. On the other hand, PCa or csPCa lesions possessed lower ADC, T1, T2 and PD values (*Figure 2*). Details of the comparison between PCa and non-PCa, clinically insignificant disease and csPCa in the training cohort are presented in *Tables 2*,*3*.

Independent risk factors for PCa and csPCa were explored by univariable and multivariable binary logistic regression analyses (*Tables 4*,*5*). In univariate regression analysis, age, fPSA, PI-RADS score, T1, T2, PD and ADC value showed statistical significance between PCa and noncancerous lesions. These factors were further incorporated into the multivariate logistic regression analysis. Finally, age, T2, ADC and PI-RADS score were identified as independent risk predictors of PCa, and a nomogram was developed based on these coefficients (*Figure 3*). As displayed in *Figure 3* and *Figure 4*, for a 73-year-old representative participant with a PI-RADS 4 lesion (ADC value of 818.48×10^{-6} mm^2/s and T2 value of 73.95 ms), the possibility of PCa was 0.953. Meanwhile, age, ADC and PI-RADS score were screened out to establish the nomogram for predicting csPCa (*Figure 5*).

Verification of the nomogram.

ROC curve analysis was used to evaluate the discrimination capacity of the established nomograms. Our models exhibited significant performance in detecting PCa and csPCa, with AUCs of 0.916 [95% confidence interval (CI): 0.877–0.956] and 0.884 (95% CI: 0.840–0.928), respectively, in the training cohort (*Figure 3*, Figure S1). For internal validation, with the method of using 1,000 bootstrap resamples, our models still displayed good discrimination, with AUCs of 0.912 (95% CI: 0.900–0.918) for PCa and 0.880 (95% CI: 0.867–0.887) for csPCa. In the external validation cohort, the AUCs of the nomogram for predicting PCa and csPCa were 0.947 (95% CI: 0.900–0.994) and 0.935 (95% CI: 0.871–0.998), respectively (*Figure 5*, Figure S1). Calibration curves (*Figures 3*,*5*, Figure S1) exhibited good concordance between the predicted probability and actual observation, which reflected the repeatability and reliability of our nomograms. In

Table 1 Patient characteristics of the training cohort and external validation cohort

Variables	Training cohort (n=243)	External validation cohort (n=80)	P value
Age (years)	70.00 (65.00, 76.00)	69.50 (64.00, 75.25)	0.685
tPSA (ng/mL)	14.47 (8.48, 32.50)	21.44 (12.68, 70.21)	0.001*
fPSA (ng/mL)	1.95 (1.29, 3.78)	2.83 (1.46, 6.65)	0.039*
f/t PSA	0.13 (0.10, 0.19)	0.10 (0.07, 0.16)	0.004*
Pathologic specimen type			0.527
Surgical specimen	107 (44.0)	32 (40.0)	
Biopsy specimen	136 (56.0)	48 (60.0)	
Pathological results			0.146
No cancer	65 (26.7)	14 (17.5)	
Gleason score 6	12 (4.9)	7 (8.8)	
Gleason score ≥7	166 (68.3)	59 (73.8)	
Lesion location			0.604
PZ	168 (69.1)	57 (73.1)	
TZ and AFS	75 (30.9)	23 (28.8)	
ADC (10 mm/s)	913.05 (809.99, 1,063.30)	921.82 (802.52, 1,161.55)	0.449
T1 (msec)	1,292.64 (1,214.20, 1,380.03)	1,269.98 (1,189.08, 1,378.11)	0.657
T2 (msec)	84.02 (78.15, 91.12)	86.43 (79.11, 94.15)	0.16
PD (pu)	81.54 (79.94, 82.76)	79.42 (77.06, 81.45)	<0.001*
PI-RADS			0.763
PI-RADS 3	60 (24.7)	23 (28.8)	
PI-RADS 4	59 (24.3)	19 (23.8)	
PI-RADS 5	124 (51.0)	38 (47.5)	

Data were expressed as median (first quartile, third quartile) or number (percentage). *, statistically significant. tPSA, total prostate-specific antigen; fPSA, free prostate-specific antigen; f/t PSA, free/total prostate-specific antigen ratio; PZ, peripheral zone; TZ, transition zone; AFS, anterior fibromuscular stroma; ADC, apparent diffusion coefficient; T1, longitudinal relaxation time; T2, transverse relaxation time; PD, proton density; PI-RADS, Prostate Imaging-Reporting and Data System.

addition, the Hosmer-Lemeshow test also demonstrated that the predictive nomograms were well calibrated, with P values of 0.427 and 0.481 for predicting PCa and 0.730 and 0.554 for predicting csPCa in the training and external validation cohorts, respectively. The DCA curves confirmed the good clinical applicability of the nomogram (*Figures 3*,*5*, Figure S1).

For the prediction of PCa, predictive values of 0.415 and 0.944 were defined as the boundary thresholds of low risk and high risk, respectively. A novel biopsy strategy was proposed based on the above criteria (*Figure 3*). For patients with PI-RADS ≥3 lesions, biopsy was not recommended when patients were at low risk of PCa (predictive value <0.415). A total of 20.2% (49/243) and 13.8% (11/80) of biopsies could be avoided with this strategy in the training and external validation cohorts, respectively. Meanwhile, the PCa missing rates were 4.5% (8/178) and 4.5% (3/66), respectively. Moreover, in patients with PI-RADS category 3 lesions, 63.3% (38/60) and 34.8% (8/23) of unnecessary biopsies could be avoided in the two cohorts.

Similarly, a biopsy strategy combining the nomogram was proposed for the prediction of csPCa, with risk thresholds of 0.308 and 0.905 (*Figure 5*). Based on this strategy, if biopsy was not performed in patients with a low risk of csPCa (predictive value 0.308), then 20.2% (49/243) and 10.0% (8/80) of biopsies could be avoided in the training

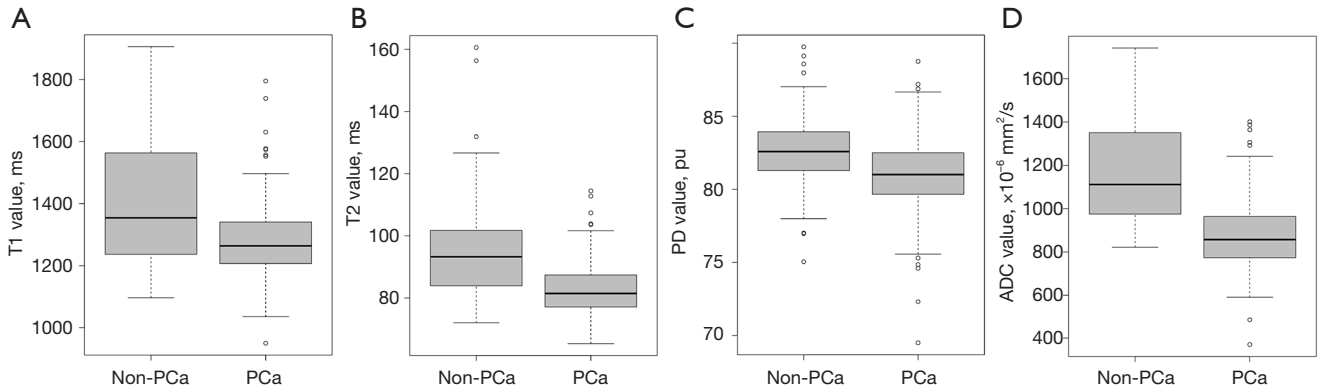

Figure 2 Box-and-whisker plots of (A) T1, (B) T2, (C) PD, and (D) ADC measurements for PCa and non-PCa. T1, longitudinal relaxation time; T2, transverse relaxation time; PD, proton density; ADC, apparent diffusion coefficient; PCa, prostate cancer.

Table 2 Characteristics of patient with and without PCa in the training cohort

Variables	Non-PCa (n=65)	PCa (n=178)	P value
Age (years)	67.00 (59.00, 71.00)	71.00 (67.00, 77.00)	<0.001*
tPSA (ng/mL)	11.32 (7.76, 16.72)	16.23 (9.29, 39.48)	<0.001*
fPSA (ng/mL)	1.66 (1.07, 2.36)	2.06 (1.36, 4.82)	0.001*
f/t PSA	0.14 (0.11, 0.22)	0.13 (0.10, 0.17)	0.203
ADC (×10^{-6} mm^2/s)	1,111.03 (974.89, 1,350.59)	857.06 (773.51, 961.95)	<0.001*
T1 (msec)	1,353.87 (1,236.63, 1,563.08)	1,263.37 (1,206.96, 1,340.17)	<0.001*
T2 (msec)	93.28 (83.91, 101.70)	81.48 (77.01, 87.37)	<0.001*
PD (pu)	82.59 (81.29, 83.94)	81.02 (79.71, 82.50)	<0.001*
PI-RADS			<0.001*
PI-RADS 3	45 (69.2)	15 (8.4)	
PI-RADS 4	13 (20.0)	46 (25.8)	
PI-RADS 5	7 (10.8)	117 (65.7)	

Data were expressed as median (first quartile, third quartile) or number (percentage). *, statistically significant. PCa, prostate cancer; tPSA, total prostate-specific antigen; fPSA, free prostate-specific antigen; f/t PSA, free/total prostate-specific antigen ratio; ADC, apparent diffusion coefficient; T1, longitudinal relaxation time; T2, transverse relaxation time; PD, proton density; PI-RADS, Prostate Imaging-Reporting and Data System.

and external validation cohorts, with csPCa missing rates of 4.8% (8/166) and 1.7% (1/59), respectively. In addition, 65.0% (39/60) and 30.4% (7/23) of unnecessary biopsies could be reduced in patients with PI-RADS category 3 lesions.

Discussion

In the current study, the capacity of quantitative parameters derived from multiparametric MRI and synthetic MRI in predicting the risk of PCa and csPCa was investigated. Our findings showed that the T1, T2, PD and ADC values were significantly lower in PCa and csPCa. Four independent risk factors for PCa were identified and incorporated into the nomogram development for PCa prediction, including PI-RADS score, ADC, T2, and age. In addition, a nomogram for csPCa prediction was also constructed based on the independent predictors of the PI-RADS score, ADC, and

Table 3 Comparison of variables between clinically insignificant disease and csPCa in the training cohort

Variables	Clinically insignificant disease (n=77)	Clinically significant prostate cancer (n=166)	P value
Age (years)	67.00 (61.00, 72.00)	71.00 (67.00, 77.00)	<0.001*
tPSA (ng/mL)	11.60 (8.00, 16.65)	16.45 (9.35, 45.77)	<0.001*
fPSA (ng/mL)	1.68 (1.11, 2.36)	2.06 (1.36, 5.42)	0.001*
f/t PSA	0.14 (0.11, 0.22)	0.13 (0.09, 0.17)	0.073
ADC ($\times10^{-6}$ mm^2/s)	1,090.51 (957.03, 1,281.97)	847.79 (763.80, 955.25)	<0.001*
T1 (msec)	1,338.75 (1,232.11, 1,523.24)	1,270.34 (1,206.08, 1,340.17)	<0.001*
T2 (msec)	91.12 (81.30, 100.43)	81.41 (76.91, 87.13)	<0.001*
PD (pu)	82.56 (80.79, 83.54)	81.02 (79.70, 82.50)	<0.001*
PI-RADS			<0.001*
PI-RADS 3	47 (61.0)	13 (7.8)	
PI-RADS 4	17 (22.1)	42 (25.3)	
PI-RADS 5	13 (16.9)	111 (66.9)	

Data were expressed as median (first quartile, third quartile) or number (percentage). *, statistically significant. csPCa, clinically significant prostate cancer; tPSA, total prostate-specific antigen; fPSA, free prostate-specific antigen; f/t PSA, free/total prostate-specific antigen ratio; ADC, apparent diffusion coefficient; T1, longitudinal relaxation time; T2, transverse relaxation time; PD, proton density; PI-RADS, Prostate Imaging-Reporting and Data System.

Table 4 Univariable and multivariable logistic regression analysis of risk factors for PCa in the training cohort

Variables	Univariable analysis		Multivariate analysis	
	Odds ratio (95% CI)	P value	Odds ratio (95% CI)	P value
Age (years)	1.079 (1.042–1.120)	<0.001*	1.067 (1.009–1.135)	0.029*
tPSA (ng/mL)	1.020 (1.007–1.040)	0.020*	0.998 (0.988–1.018)	0.694
fPSA (ng/mL)	1.204 (1.063–1.443)	0.020*	1.099 (0.961–1.490)	0.483
f/t PSA	0.300 (0.015–6.531)	0.431		
ADC ($\times10^{-6}$ mm^2/s)	0.993 (0.991–0.995)	<0.001*	0.997 (0.994–1.000)	0.037*
T1 (msec)	0.995 (0.9923–0.997)	<0.001*	1.003 (0.999–1.007)	0.179
T2 (msec)	0.907 (0.877–0.935)	<0.001*	0.931 (0.872–0.985)	0.021*
PD (pu)	0.785 (0.691–0.882)	0.001*	0.901 (0.736–1.098)	0.302
PI-RADS				
PI-RADS 3	–		–	
PI-RADS 4	10.616 (4.675–25.711)	<0.001*	9.579 (3.492–28.945)	<0.001*
PI-RADS 5	50.143 (20.313–141.180)	<0.001*	20.139 (6.743–68.442)	<0.001*

*, statistically significant. PCa, prostate cancer; CI, confidence interval; tPSA, total prostate-specific antigen; fPSA, free prostate-specific antigen; f/t PSA, free/total prostate-specific antigen ratio; ADC, apparent diffusion coefficient; T1, longitudinal relaxation time; T2, transverse relaxation time; PD, proton density; PI-RADS, Prostate Imaging-Reporting and Data System.

Table 5 Univariable and multivariable logistic regression analysis of risk factors for csPCa in the training cohort

Variables	Univariable analysis		Multivariate analysis	
	Odds ratio (95% CI)	P value	Odds ratio (95% CI)	P value
Age (years)	1.075 (1.039–1.114)	<0.001*	1.052 (1.002–1.108)	0.047*
tPSA (ng/mL)	1.024 (1.010–1.045)	0.006*	1.001 (0.990–1.030)	0.908
fPSA (ng/mL)	1.217 (1.077–1.443)	0.010*	1.094 (0.940–1.416)	0.456
f/t PSA	0.158 (0.009–2.862)	0.207		
ADC ($\times 10^{-6}$ mm^2/s)	0.993 (0.991–0.995)	<0.001*	0.997 (0.994–0.999)	0.016*
T1 (msec)	0.995 (0.9923–0.997)	<0.001*	1.002 (0.998–1.006)	0.278
T2 (msec)	0.920 (0.892–0.946)	<0.001*	0.956 (0.904–1.005)	0.092
PD (pu)	0.802 (0.711–0.895)	<0.001*	0.898 (0.747–1.0717)	0.237
PI-RADS				
PI-RADS 3	–		–	
PI-RADS 4	8.932 (3.985–21.250)	<0.001*	6.469 (2.518–17.659)	<0.001*
PI-RADS 5	30.870 (13.799–74.732)	<0.001*	10.179 (3.861–28.673)	<0.001*

*, statistically significant. csPCa, clinically significant prostate cancer; CI, confidence interval; tPSA, total prostate-specific antigen; fPSA, free prostate-specific antigen; f/t PSA, free/total prostate-specific antigen ratio; ADC, apparent diffusion coefficient; T1, longitudinal relaxation time; T2, transverse relaxation time; PD, proton density; PI-RADS, Prostate Imaging-Reporting and Data System.

age. The high clinical application value of the nomograms was affirmed by the AUC, calibration curves and decision curve.

Current guidelines suggest that lesions with PI-RADS ≥3 have an intermediate to high probability of being PCa, and biopsies are recommended (6). Nonetheless, a previous multicentre randomized controlled study reported that the negative rates of transperineal targeted biopsy for patients with PI-RADS 3, PI-RADS 4 and 5 were 67%, 31% and 6%, respectively (20). Consistently, 68.7%, 19.2% and 4.3% of biopsies of PI-RADS 3, 4 and 5 lesions, respectively, were negative in our study. Such potential false-positive biopsy results of PI-RADS ≥3 lesions may lead urologists to suspect that the biopsy fails to target the actual lesion and may also induce anxiety in patients. Several previous studies attempted to reduce the adverse impacts of personal subjectivity on the PI-RADS score by adding extra objective and precise clinical indicators (21-24). Zhou *et al.* (23) combined PI-RADS and the prostate health index (PHI) to establish a nomogram for PCa detection, which showed satisfactory performance, with AUCs of 0.902 and 0.869 in the training and validation cohorts, respectively. The study of Deniffel *et al.* (24) demonstrated that the number of unnecessary prostate biopsies can be safely reduced with the joint model of PI-RADS and prostate specific antigen density (PSAD). However, diseases such as urinary tract infection or the therapeutic procedure of urinary catheter placement might influence the level of these PSA-related indices and thus may affect the diagnosis of PCa.

As the basic intrinsic properties of MRI physics, quantitative T1, T2, and PD values obtained from synthetic MRI can provide us information about tissue composition, such as macromolecule concentration and tissue water content, and they would not be influenced by MRI scanners or scanning parameters at a given field strength (15). Several studies have demonstrated the utility of T1, T2 and PD mapping in the quantitative evaluation of PCa (12,25,26). In our study, we incorporated the objective and quantitative parameters derived from synthetic MRI and ADC mapping. The results indicated that the T1, T2 and PD values of PCa were lower than those in noncancer tissue, as were those of csPCa compared to clinically insignificant diseases. In addition, the T2 value was an independent risk factor for PCa. T2 values are regarded as biomarkers to reflect the amount of water content, cell density, and tissue composition. According to the literature (26), low T2 values in PCa might be attributed to the loss of glandular architecture and its corresponding secretory function.

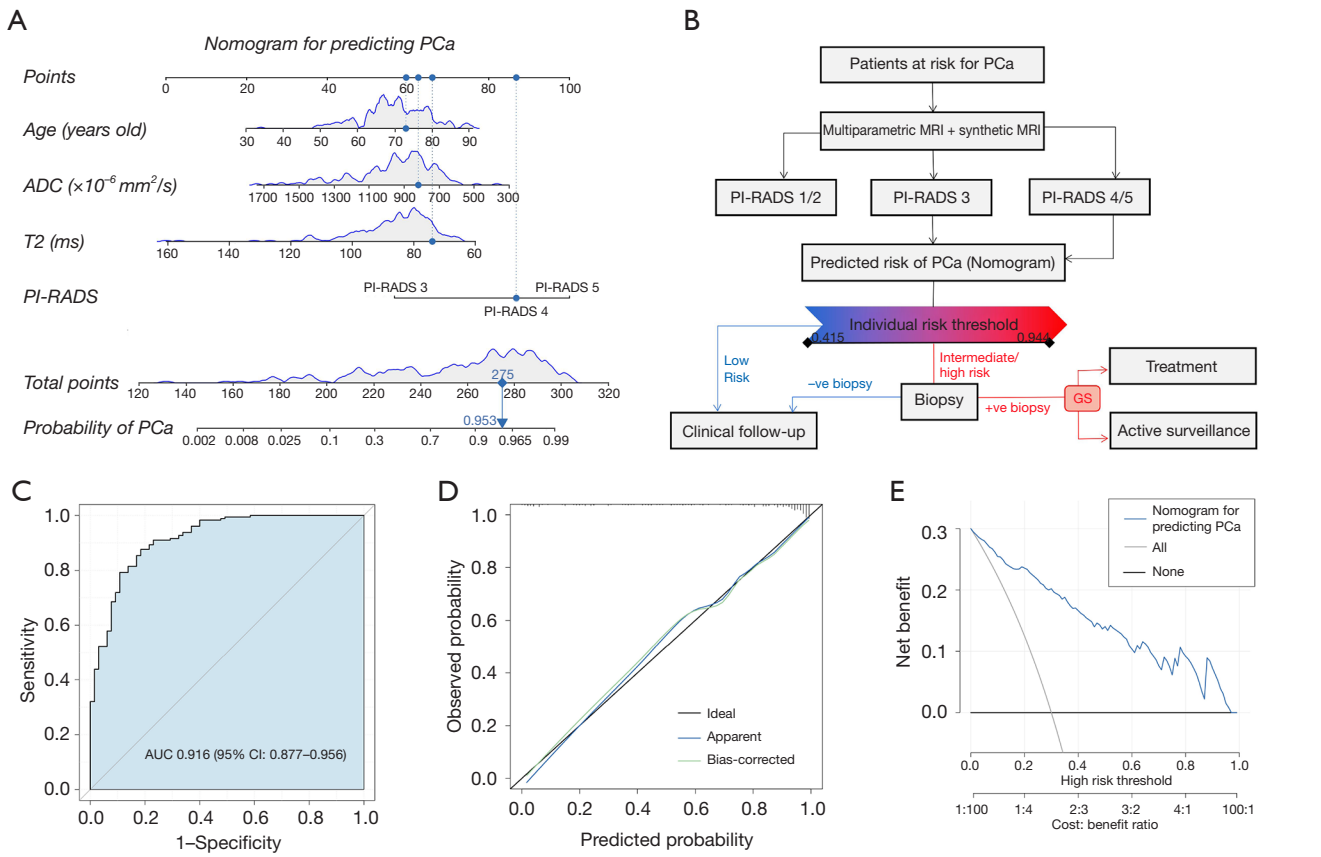

Figure 3 Nomogram for the detection of PCa and performance evaluation in the training cohort. (A) Nomogram; (B) biopsy strategy combining the nomogram; (C) receiver operating characteristic curve; (D) calibration curve; (E) decision curve. Instructions: the value for each factor (age, T2 value, ADC value, PI-RADS score) corresponds to the point vertically above the below scale. The values are added together to determine the total points, which then correspond to the estimated risk of PCa shown on the scale at the bottom. PCa, prostate cancer; ADC, apparent diffusion coefficient; T2, transverse relaxation time; PI-RADS, Prostate Imaging Reporting and Data System; MRI, magnetic resonance imaging; GS, Gleason score; AUC, area under the curve; CI, confidence interval.

Lower ADC in cancer is a well-documented phenomenon related to diminished water self-diffusivity. Our study also demonstrated a lower ADC value in PCa as well as csPCa, and ADC was found to be an independent predictor of either PCa or csPCa. The possible explanation for this finding might be attributed to the increase in cellular density in PCa and csPCa, which reduces the extracellular space and restricts the movement of water protons (27).

We then constructed a nomogram for predicting PCa based on the selected independent predictive factors, including PI-RADS score, T2, ADC and age. Although several nomograms for PCa diagnosis were established incorporating PI-RADS, ADC and other clinical risk factors, the combination with the T2 value has not yet been constructed (23,28-30). The nomogram in this study showed good diagnostic accuracy for the diagnosis of PCa in all the training and external validation cohorts, with AUCs of 0.916 and 0.947, respectively. The calibration curves and decision curves for the two cohorts demonstrated that the established nomogram was reliable for clinical application. Nonetheless, although significant differences were found between csPCa and clinically insignificant diseases with regard to the quantitative parameters obtained from synthetic MRI, none of the synthetic MRI-derived indices were found to be independent predictors of csPCa. In the study by Yu *et al.* (26), T2 was a significant univariate predictor for differentiating between histologically proven high- or intermediate-grade tumours and low-grade tumours, and the combination of ADC and T2 produced an AUC of 0.830. However, the study results of Panda *et al.* (25)

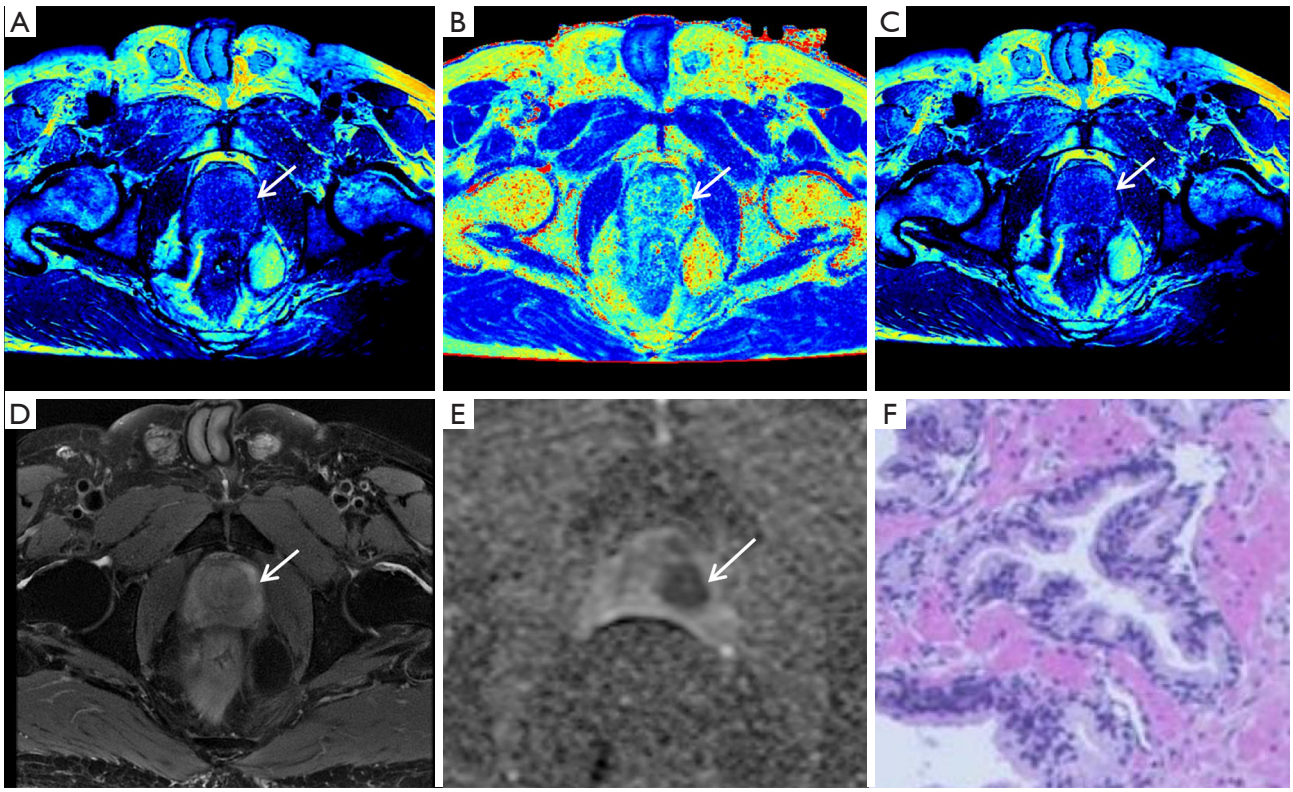

Figure 4 Multiparametric MRI and synthetic MRI images of a 73-year-old representative participant. (A-C) Synthetic MRI-derived T1, T2 and PD maps; (D) axial T2-weighted image; (E) ADC map; (F) pathological image (H&E, ×200 magnification). A PI-RADS 4 lesion was located in the left transition zone (arrows), with the ADC value of 818.48×10^{-6} mm^2/s and T2 value of 73.95 ms. According to the nomogram, the possibility of PCa diagnosis was 0.953. Final pathological diagnosis confirmed it to be PCa with Gleason score 3+4. MRI, magnetic resonance imaging; T1, longitudinal relaxation time; T2, transverse relaxation time; PD, proton density; ADC, apparent diffusion coefficient; H&E, hematoxylin-eosin staining; PI-RADS, Prostate Imaging Reporting and Data System; PCa, prostate cancer.

indicated that T1 but not T2 was an independent risk factor. Such discrepancies among studies might be due to disparities in the included populations, which indicates the need for further investigation with larger samples.

It is worth mentioning that we proposed a novel biopsy strategy based on the predicted value generated from the nomograms, with the aim of reducing unnecessary biopsies. When focusing specifically on detecting all pathological grades of PCa, prostate biopsy was not recommended when the predicted value was lower than 0.415 in patients with PI-RADS ≥3 lesions. By applying this criterion, 20.2% and 13.8% of biopsies can be avoided in the training and external validation cohorts, with a low risk of missing PCa (4.5% and 4.5%, respectively). In addition, PI-RADS 3 has always been considered an imaging grey zone for PCa. The most troubling hurdle of the current biopsy decision strategies based on PI-RADS is the different PCa detection rate in PI-RADS 3 lesions. With our biopsy strategy, 63.3% and 34.8% of unnecessary biopsies could be avoided for men with PI-RADS category 3 lesions in the two cohorts, which might partly help to address problems that plague clinicians. Our biopsy strategy does not require much additional scan time or intravenous contrast. The biopsy strategy focusing on detecting csPCa (with a low-risk threshold of 0.308) also showed clinical benefit, with biopsy avoidance rates of 20.2% and 10.0% and corresponding csPCa miss rates of 4.8% and 1.7% for patients with PI-RADS ≥3 lesions in the training and external validation cohorts, respectively. Apart from that, the nomograms have additional advantages of being intuitive and user-friendly, which may assist urologists in making better biopsy decisions.

There are some limitations in this study. First, the ISUP grade group of PCa was determined either by biopsy

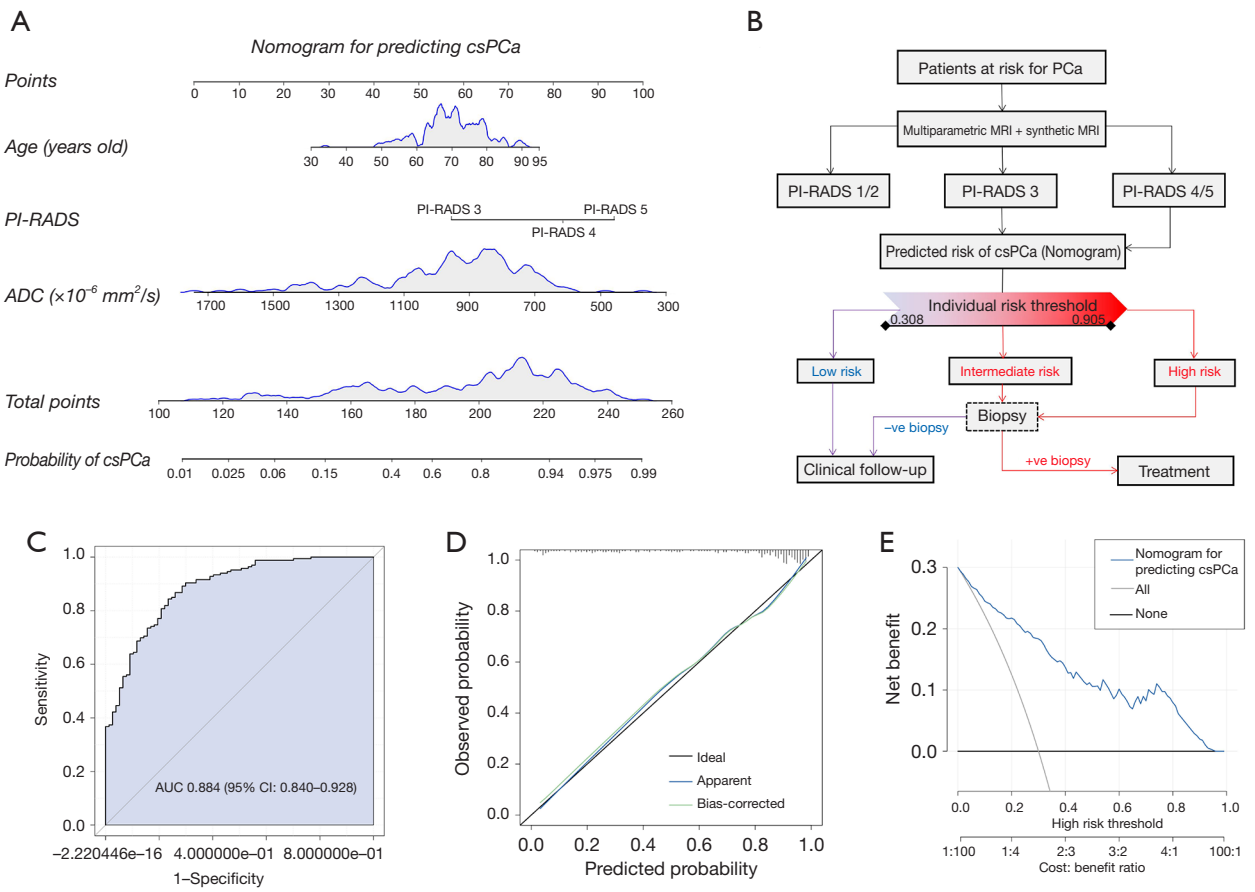

Figure 5 Nomogram for the detection of csPCa and performance evaluation in the training cohort. (A) Nomogram; (B) biopsy strategy combining the nomogram; (C) receiver operating characteristic curve; (D) calibration curve; (E) decision curve. csPCa, clinically significant prostate cancer; PI-RADS, Prostate Imaging Reporting and Data System; ADC, apparent diffusion coefficient; MRI, magnetic resonance imaging; AUC, area under the curve; CI, confidence interval.

or surgery specimens, and the biopsy results have the possibility of under- or overestimating the Gleason score in comparison to the surgical results. Second, significant differences were found between the two institutions with regard to tPSA, fPSA, f/t PSA, and PD value on account of the bicentric population variation. Fortunately, the parameters mentioned above were not included in the nomogram construction. Third, although eligible patients for this study were recruited from two medical centres, the sample size of this study was relatively small. Multicentre evaluation with a larger sample for the established nomograms is still needed in future studies.

Conclusions

The nomograms incorporating parameters derived from multiparametric MRI and synthetic MRI could efficiently predict the risk of PCa and csPCa. An effective biopsy strategy combining the developed nomogram can assist in reducing the number of unnecessary biopsies in patients with PI-RADS ≥3 lesions.

Acknowledgments

Funding: This work was supported by the National Natural Science Foundation of China (Nos. 82071989, 82372075, and 82371911).

Footnote

Reporting Checklist: The authors have completed the TRIPOD reporting checklist. Available at https://qims.

amegroups.com/article/view/10.21037/qims-24-1072/rc

Conflicts of Interest: All authors have completed the ICMJE uniform disclosure form (available at https://qims.amegroups.com/article/view/10.21037/qims-24-1072/coif). All authors report that this work was supported by the National Natural Science Foundation of China (Nos. 82071989, 82372075, and 82371911). The authors have no other conflicts of interest to declare.

Ethical Statement: The authors are accountable for all aspects of the work in ensuring that questions related to the accuracy or integrity of any part of the work are appropriately investigated and resolved. The study was conducted in accordance with the Declaration of Helsinki (as revised in 2013). The whole study was mainly designed and developed in The First Affiliated Hospital of Sun Yat-Sen University and Ethical approval was obtained from the Ethics Committee of The First Affiliated Hospital of Sun Yat-Sen University (2023; approval No. 094). Both participating medical centres were informed and agreed with the study. The informed consent was taken from all individual participants.

References

1. Bray F, Laversanne M, Sung H, Ferlay J, Siegel RL, Soerjomataram I, Jemal A. Global cancer statistics 2022: GLOBOCAN estimates of incidence and mortality worldwide for 36 cancers in 185 countries. CA Cancer J Clin 2024;74:229-63.
2. Finati M, Davis M, Stephens A, Chiarelli G, Cirulli GO, Morrison C, Affas R, Sood A, Buffi N, Lughezzani G, Briganti A, Montorsi F, Carrieri G, Rogers C, Vickers AJ, Abdollah F. The Role of Baseline Prostate-specific Antigen Value Prior to Age 60 in Predicting Lethal Prostate Cancer: Analysis of a Contemporary North American Cohort. Eur Urol Oncol 2024. [Epub ahead of print]. doi: 10.1016/j.euo.2024.06.014.
3. Mayer R, Turkbey B, Choyke P, Simone CB 2nd. Combining and analyzing novel multi-parametric magnetic resonance imaging metrics for predicting Gleason score. Quant Imaging Med Surg 2022;12:3844-59.
4. Fazekas T, Shim SR, Basile G, Baboudjian M, Kói T, Przydacz M, Abufaraj M, Ploussard G, Kasivisvanathan V, Rivas JG, Gandaglia G, Szarvas T, Schoots IG, van den Bergh RCN, Leapman MS, Nyirády P, Shariat SF, Rajwa P. Magnetic Resonance Imaging in Prostate Cancer Screening: A Systematic Review and Meta-Analysis. JAMA Oncol 2024;10:745-54.
5. Turkbey B, Rosenkrantz AB, Haider MA, Padhani AR, Villeirs G, Macura KJ, Tempany CM, Choyke PL, Cornud F, Margolis DJ, Thoeny HC, Verma S, Barentsz J, Weinreb JC. Prostate Imaging Reporting and Data System Version 2.1: 2019 Update of Prostate Imaging Reporting and Data System Version 2. Eur Urol 2019;76:340-51.
6. Padhani AR, Barentsz J, Villeirs G, Rosenkrantz AB, Margolis DJ, Turkbey B, Thoeny HC, Cornud F, Haider MA, Macura KJ, Tempany CM, Verma S, Weinreb JC. PI-RADS Steering Committee: The PI-RADS Multiparametric MRI and MRI-directed Biopsy Pathway. Radiology 2019;292:464-74.
7. Bjurlin MA, Carroll PR, Eggener S, Fulgham PF, Margolis DJ, Pinto PA, Rosenkrantz AB, Rubenstein JN, Rukstalis DB, Taneja SS, Turkbey B. Update of the Standard Operating Procedure on the Use of Multiparametric Magnetic Resonance Imaging for the Diagnosis, Staging and Management of Prostate Cancer. J Urol 2020;203:706-12.
8. Mottet N, van den Bergh RCN, Briers E, Van den Broeck T, Cumberbatch MG, De Santis M, et al. EAU-EANM-ESTRO-ESUR-SIOG Guidelines on Prostate Cancer-2020 Update. Part 1: Screening, Diagnosis, and Local Treatment with Curative Intent. Eur Urol 2021;79:243-62.
9. Westphalen AC, McCulloch CE, Anaokar JM, Arora S, Barashi NS, Barentsz JO, et al. Variability of the Positive Predictive Value of PI-RADS for Prostate MRI across 26 Centers: Experience of the Society of Abdominal Radiology Prostate Cancer Disease-focused Panel. Radiology 2020;296:76-84.
10. Stolk TT, de Jong IJ, Kwee TC, Luiting HB, Mahesh SVK, Doornweerd BHJ, Willemse PM, Yakar D. False positives in PIRADS (V2) 3, 4, and 5 lesions: relationship with reader experience and zonal location. Abdom Radiol

(NY) 2019;44:1044-51.
11. Tian H, Ding Z, Wu H, Yang K, Song D, Xu J, Dong F. Assessment of elastographic Q-analysis score combined with Prostate Imaging-Reporting and Data System (PI-RADS) based on transrectal ultrasound (TRUS)/multi-parameter magnetic resonance imaging (MP-MRI) fusion-guided biopsy in differentiating benign and malignant prostate. Quant Imaging Med Surg 2022;12:3569-79.
12. Cui Y, Han S, Liu M, Wu PY, Zhang W, Zhang J, Li C, Chen M. Diagnosis and Grading of Prostate Cancer by Relaxation Maps From Synthetic MRI. J Magn Reson Imaging 2020;52:552-64.
13. Zhan T, Yi C, Lang Y. Predicting efficacy of neoadjuvant chemotherapy in breast cancer patients with synthetic magnetic resonance imaging method MAGiC: An observational cohort study. Eur J Radiol 2024;179:111666.
14. Zhan T, Dai J, Li Y. Noninvasive identification of HER2-zero, -low, or -overexpressing breast cancers: Multiparametric MRI-based quantitative characterization in predicting HER2-low status of breast cancer. Eur J Radiol 2024;177:111573.
15. Cai Q, Wen Z, Huang Y, Li M, Ouyang L, Ling J, Qian L, Guo Y, Wang H. Investigation of Synthetic Magnetic Resonance Imaging Applied in the Evaluation of the Tumor Grade of Bladder Cancer. J Magn Reson Imaging 2021;54:1989-97.
16. Onishi S, Yamasaki F, Akiyama Y, Kawahara D, Amatya VJ, Yonezawa U, Taguchi A, Ozono I, Khairunnisa NI, Takeshima Y, Horie N. Usefulness of synthetic MRI for differentiation of IDH-mutant diffuse gliomas and its comparison with the T2-FLAIR mismatch sign. J Neurooncol 2024. [Epub ahead of print]. doi: 10.1007/s11060-024-04794-0.
17. Zhang P, Yang J, Shu Y, Cheng M, Zhao X, Wang K, Lu L, Xing Q, Niu G, Meng L, Wang X, Zhou L, Zhang X. The value of synthetic MRI in detecting the brain changes and hearing impairment of children with sensorineural hearing loss. Front Neurosci 2024;18:1365141.
18. Park SY. Nomogram: An analogue tool to deliver digital knowledge. J Thorac Cardiovasc Surg 2018;155:1793.
19. Wu D, Jiang K, Li H, Zhang Z, Ba R, Zhang Y, Hsu YC, Sun Y, Zhang YD. Time-Dependent Diffusion MRI for Quantitative Microstructural Mapping of Prostate Cancer. Radiology 2022;303:578-87.
20. Kasivisvanathan V, Rannikko AS, Borghi M, Panebianco V, Mynderse LA, Vaarala MH, et al. MRI-Targeted or Standard Biopsy for Prostate-Cancer Diagnosis. N Engl J Med 2018;378:1767-77.
21. Zhou Y, Fu Q, Shao Z, Qi W, Zhong M, Lv G, Jiang Z, Zhu M, Wang W, Shi B, Chen S, Zhu Y. The function of Prostate Health Index in detecting clinically significant prostate cancer in the PI-RADS 3 population: a multicenter prospective study. World J Urol 2023;41:455-61.
22. Wang C, Yuan L, Shen D, Zhang B, Wu B, Zhang P, Xiao J, Tao T. Combination of PI-RADS score and PSAD can improve the diagnostic accuracy of prostate cancer and reduce unnecessary prostate biopsies. Front Oncol 2022;12:1024204.
23. Zhou Y, Fu Q, Shao Z, Zhang K, Qi W, Geng S, Wang W, Cui J, Jiang X, Li R, Zhu Y, Chen S, Shi B. Nomograms Combining PHI and PI-RADS in Detecting Prostate Cancer: A Multicenter Prospective Study. J Clin Med 2023;12:339.
24. Deniffel D, Healy GM, Dong X, Ghai S, Salinas-Miranda E, Fleshner N, Hamilton R, Kulkarni G, Toi A, van der Kwast T, Zlotta A, Finelli A, Perlis N, Haider MA. Avoiding Unnecessary Biopsy: MRI-based Risk Models versus a PI-RADS and PSA Density Strategy for Clinically Significant Prostate Cancer. Radiology 2021;300:369-79.
25. Panda A, Obmann VC, Lo WC, Margevicius S, Jiang Y, Schluchter M, Patel IJ, Nakamoto D, Badve C, Griswold MA, Jaeger I, Ponsky LE, Gulani V. MR Fingerprinting and ADC Mapping for Characterization of Lesions in the Transition Zone of the Prostate Gland. Radiology 2019;292:685-94.
26. Yu AC, Badve C, Ponsky LE, Pahwa S, Dastmalchian S, Rogers M, Jiang Y, Margevicius S, Schluchter M, Tabayoyong W, Abouassaly R, McGivney D, Griswold MA, Gulani V. Development of a Combined MR Fingerprinting and Diffusion Examination for Prostate Cancer. Radiology 2017;283:729-38.
27. Park SB. Quantitative relaxation maps from synthetic MRI for prostate cancer. Acta Radiol 2022;63:982-3.
28. Xie W, Xu Z, Qiu Y, Ye W, Zhang Z, Wang C, Zang J. A Novel Nomogram Combined the Aggregate Index of Systemic Inflammation and PIRADS Score to Predict the Risk of Clinically Significant Prostate Cancer. Biomed Res Int 2023;2023:9936087.
29. Hu C, Sun J, Xu Z, Zhang Z, Zhou Q, Xu J, Chen H, Wang C, Ouyang J. Development and external validation of a novel nomogram to predict prostate cancer in biopsy-

naïve patients with PSA <10 ng/ml and PI-RADS v2.1 = 3 lesions. Cancer Med 2023;12:2560-71.
30. Zhou Z, Liang Z, Zuo Y, Zhou Y, Yan W, Wu X, Ji Z, Li H, Hu M, Ma L. Development of a nomogram combining multiparametric magnetic resonance imaging and PSA-related parameters to enhance the detection of clinically significant cancer across different region. Prostate 2022;82:556-65.

Cite this article as: Chen Y, Lin J, Cao W, Meng T, Ling J, Wen Z, Kong L, Qian L, Guo Y, Zhang W, Wang H. Optimizing prostate biopsy decision-making for patients with Prostate Imaging-Reporting and Data System (PI-RADS) ≥3 lesions: novel magnetic resonance imaging (MRI)-based nomograms. Quant Imaging Med Surg 2024;14(12):8196-8210. doi: 10.21037/qims-24-1072